This article was downloaded by: [National Chiao Tung University 國立交通大學]
On: 28 April 2014, At: 14:21
Publisher: Taylor & Francis
Informa Ltd Registered in England and Wales Registered Number: 1072954 Registered office: Mortimer House, 37-41 Mortimer Street, London W1T 3JH, UK

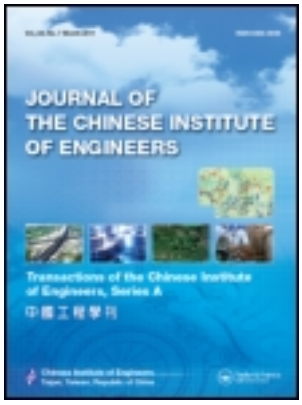

Journal of the Chinese Institute of Engineers
Publication details, including instructions for authors and subscription information:
http://www.tandfonline.com/loi/tcie20

Optimal variable speed-limit control under abnormal traffic conditions

Yu-Chiun Chiou [a], Yen-Fei Huang [a] & Po-Cheng Lin [a]
[a] Institute of Traffic and Transportation, National Chiao Tung University, Taipei, Taiwan
Published online: 21 Mar 2012.

To cite this article: Yu-Chiun Chiou, Yen-Fei Huang & Po-Cheng Lin (2012) Optimal variable speed-limit control under abnormal traffic conditions, Journal of the Chinese Institute of Engineers, 35:3, 299-308, DOI: 10.1080/02533839.2012.655472

To link to this article: http://dx.doi.org/10.1080/02533839.2012.655472

PLEASE SCROLL DOWN FOR ARTICLE

Taylor & Francis makes every effort to ensure the accuracy of all the information (the "Content") contained in the publications on our platform. However, Taylor & Francis, our agents, and our licensors make no representations or warranties whatsoever as to the accuracy, completeness, or suitability for any purpose of the Content. Any opinions and views expressed in this publication are the opinions and views of the authors, and are not the views of or endorsed by Taylor & Francis. The accuracy of the Content should not be relied upon and should be independently verified with primary sources of information. Taylor and Francis shall not be liable for any losses, actions, claims, proceedings, demands, costs, expenses, damages, and other liabilities whatsoever or howsoever caused arising directly or indirectly in connection with, in relation to or arising out of the use of the Content.

This article may be used for research, teaching, and private study purposes. Any substantial or systematic reproduction, redistribution, reselling, loan, sub-licensing, systematic supply, or distribution in any form to anyone is expressly forbidden. Terms & Conditions of access and use can be found at http://www.tandfonline.com/page/terms-and-conditions

Journal of the Chinese Institute of Engineers
Vol. 35, No. 3, April 2012, 299–308

Taylor & Francis
Taylor & Francis Group

Optimal variable speed-limit control under abnormal traffic conditions

Yu-Chiun Chiou*, Yen-Fei Huang and Po-Cheng Lin

Institute of Traffic and Transportation, National Chiao Tung University, Taipei, Taiwan

(*Received 25 June 2010; final version received 23 November 2010*)

Application of variable speed-limit (VSL) control has become promising in managing incidents in the context of intelligent highway systems, wherein advanced VSL signs are densely placed along the roadways. This paper aims to develop a genetic-fuzzy-logic- controller (GFLC)-based VSL control model with an objective function to enhance both safety and throughput efficiency at incident sites. In order to evaluate the performance of learned logic rules and tuned membership function, a revised cell transmission model is proposed, which is validated with field traffic data. The results indicate that the proposed VSL control model can effectively curtail crash likelihood while only slightly decreasing the throughput efficiency under different tested incident cases. It suggests that our proposed GFLC-based VSL control model is promising for practical applications.

Keywords: cell transmission model; genetic fuzzy logic controller; variable speed-limit control

Downloaded by [National Chiao Tung University] at 14:21 28 April 2014

1. Introduction

The abrupt reduction of roadway capacity at incident sites can generate manifest shockwaves along which apparent speed variations emerge. Such speed variations are due to normal speed traffic (free-flow phase) joining the gridlock traffic (congested phase), which not only decreases the roadway throughput capability but also induces accidents. Recently, different variable speed-limit (VSL) control algorithms have been proposed to eliminate, or, at least, to reduce the sizes of such shockwaves. Traditionally, VSL systems are used in planned or anticipated incidents such as work zones; however, VSL control systems have become promising in managing unexpected incidents in the context of intelligent highway systems wherein advanced VSL signs are densely placed along the roadways. Therefore, it is a challenging issue to determine the optimal VSL control schemes for such unexpected incidents along roadways with dense VSL signs.

In the literature, to evaluate the performance of VSL control systems, the following two indices are typically used: (1) efficiency, represented by minimizing delay or maximizing throughput (i.e., total number of vehicles passing through the incident site) during the evaluation period and (2) safety, represented by minimizing crash potential (Lee *et al*. 2006) or crash likelihood (Abdey-Aty *et al*. 2006). The VSL control algorithms can be roughly divided into microscopic and macroscopic categories, depending on how traffic features are depicted. In the microscopic category, most VSL algorithms utilize microscopic traffic simulators with consideration of crash likelihood and throughput efficiency. For instance, Yadlapati and Park (2004) proposed and evaluated three VSL control logics at work zones by a microscopic traffic simulator – VISSIM. Lin *et al*. (2004) proposed and evaluated two online VSL control algorithms at highway work zones by a microscopic traffic simulator – CORSIM-RTE. Lee *et al*. (2004, 2006) examined three VSL control strategies by using a microscopic traffic simulator – PARAMICS to evaluate the proposed control logics based on short-term variation of traffic flow characteristics. Abdey-Aty *et al*. (2005, 2006) also employed PARAMICS to investigate the changes in crash likelihood function under 12 logically derived VSL control strategies. Kang and Chang (2006) proposed an optimal time-of-day speed limit control (TOD SL) model with core logic to divide the entire day of operations into a number of control periods based on historical traffic patterns and to determine an optimal speed-limit control strategy for accommodating the time-varying traffic conditions within each control period. The performance of the proposed model, in terms of operational efficiency and traffic safety, was evaluated by CORSIM. In the macroscopic category, on the other hand, most VSL algorithms normally utilize macroscopic traffic simulators and focus only on throughput efficiency because the crash

*Corresponding author. Email: ycchiou@mail.nctu.edu.tw

ISSN 0253–3839 print/ISSN 2158–7299 online
© 2012 The Chinese Institute of Engineers
http://dx.doi.org/10.1080/02533839.2012.655472
http://www.tandfonline.com

Downloaded by [National Chiao Tung University] at 14:21 28 April 2014

potential due to speed variation and interaction among vehicles can hardly be analyzed or simulated. For example, Breton *et al.* (2002) and Hegyi *et al.* (2005) respectively proposed a predictive coordinated ramp metering and a VSL model to extend the control mechanism of ramp metering to increase the outflow, subject to the maximum on-ramp queue length constraint. A macroscopic traffic simulator, METANET, was used to predict the traffic demand and to evaluate the model performance.

Enhancement of safety and throughput efficiency should be regarded as the major purposes for implementing VSL control systems; thus, it is crucial to develop a sophisticated VSL control model that can simultaneously enhance both indexes or optimally compromise both. Most of the existing VSL control algorithms, however, subjectively determine the reduction of speed limit without any optimization mechanism; thus, the performance of speed-limit control cannot be guaranteed. To remedy these shortcomings, this paper aims to develop a genetic-fuzzy-logic-controller (GFLC)-based model for optimal VSL controls with consideration of throughput and safety. The GFLC model with an iterative evolution algorithm, proposed by Chiou and Lan (2005), is employed to optimally determine the reduction of speed limit according to real-time upstream traffic conditions and severity of incidents. In order to evaluate the performance of learned logic rules and tuned membership function, this study further revised the cell transmission model (CTM), a mesoscopic model proposed by Daganzo (1994, 1995). The fundamental diagrams and the equations governing traffic moving from one cell to another are revised to account for the capacity reduction at incident sites and the effects of speed-limit change on the traffic behavior. We validate the revised CTM model with different real incident cases to accurately replicate freeway traffic behavior under normal and abnormal conditions.

The remaining parts are organized as follows. Section 2 briefly introduces the methods used in this paper, including GFLC and the revised CTM model. Section 3 presents the validation of the revised CTM model in replicating the real traffic hydrodynamic behavior. The performance of the proposed VSL control model is tested by various severity degrees of incidents in Section 4. Finally, concluding remarks and suggestions for future research follow.

2. Methods

2.1. *The GFLC model*

To develop a self-learning GFLC-based VLS control model, the iterative GFLC model, proposed by Chiou and Lan (2005), is adopted in this paper. The GFLC model considers three state variables: flow rate, speed, and incident severity (represented by the percentage of lanes closed due to the incident). The control variable is to determine the optimal speed-limit increment for the VLS signs upstream of the incident sites.

To explain the core logic of the proposed VSL control mechanism, we consider a two-lane freeway with speed limit of 110 km/h under normal conditions. This speed limit is prevailing on Taiwan's freeways. The VSL signs are assumed equally spaced, every 1 km, along the freeway. Suppose an incident takes place causing one lane to close, such that the traffic can safely pass through at an average speed of 50 km/h. Then, the proposed model is to determine the optimal speed-limit increments (e.g., 10 km/h) such that the VSL sign right at the incident site will display 50 km/h and that the consecutive upstream VSL signs will display incrementally varying speed limits from 60 km/h up until 110 km/h. In this case, at least seven different VSL signs will be activated with displays of 50, 60, 70, 80, 90, 100, and 110 km/h, respectively. If the optimal speed-limit increment is 20 km/h, then at least four VSL signs will be activated, with displays of 50, 70, 90, and 110 km/h, respectively. In this study, the optimal speed-limit increment will be updated every 5 min. It should be mentioned that even for the same incident, our proposed VSL control will vary, as time evolves, to account for the time-dependent traffic and incident updates such as partial lanes restored to traffic.

To guide the learning process, crash likelihood (CL) and throughput (TT) are used to evaluate the performance of our proposed VSL control model. In this study, CL is calculated by the Abdey-Aty *et al.* (2005) formulas and TT is measured by total number of vehicles passing through the incident site during the evaluation period. The objective function of the proposed VSL control model is defined as

$$E = \alpha\left(\frac{\mathrm{CL} - \mathrm{CL}_{\min})}{\mathrm{CL}_{\max} - \mathrm{CL}_{\min}}\right) + (1-\alpha)\left(\frac{\mathrm{TT}_{\max} - \mathrm{TT}}{\mathrm{TT}_{\max} - \mathrm{TT}_{\min}}\right) \tag{1}$$

where, E is the objective value. α is the weight of CL representing the relative importance of safety over efficiency. $\mathrm{CL}_{\max}$ and $\mathrm{CL}_{\min}$ represent the maximum and minimum values of CL, respectively. $\mathrm{TT}_{\max}$ and $\mathrm{TT}_{\min}$ represent the maximum and minimum values of TT, respectively. With proper settings of maximal and minimal values of CL and TT, E will always remain positive and nonzero during the GA evolutionary process. In addition, according to Equation (1), the smaller value of E represents the lower crash likelihood

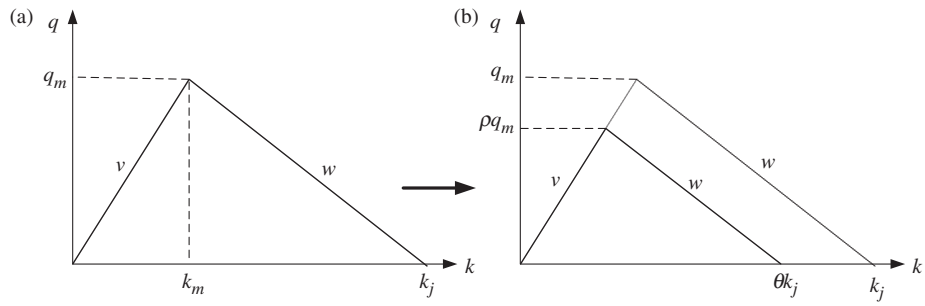

Figure 1. q-k diagrams for (a) normal and (b) lane-closure segments.

and/or larger traffic throughput. Thus, the fitness value (F) of the GFLC model is set as $F=1/E$.

2.2. *Revised cell transmission model*

To facilitate the learning process of the proposed model, an efficient traffic simulator is necessary to evaluate the performance of a set of selected logic rules and tuned membership functions in a very short period. Obviously, the learning time of the proposed model will rapidly grow intractably if a microscopic traffic simulator is used. However, if a macroscopic traffic simulator is adopted, it is impossible to evaluate the safety index due to the lack of information of interactive behavior among vehicles. Thus, a mesoscopic traffic simulator can be considered. CTM, proposed by Daganzo (1994, 1995) to simulate traffic hydrodynamic behavior in a mesoscopic manner, uses several simple equations to govern traffic movements along the roadway represented by a series of equal-length cells. These equations are expressed as follows:

$$n_i(t+1) = n_i(t) + y_i(t) - y_{i+1}(t), \tag{2}$$

$$y_i(t) = \min\{n_{i-1}(t), q_{mi}(t), \beta[N_i(t) - n_i(t)]\}, \tag{3}$$

$$\beta = \begin{cases} 1, & n_{i-1}(t) \le q_{mi}(t) \\ \dfrac{w}{v}, & n_{i-1}(t) \ge q_{mi}(t) \end{cases}, \tag{4}$$

where, $n_i(t)$ represents the number of vehicles in cell i at time t. $y_i(t)$ represents the number of vehicles flowing into cell i at time t. $q_{mi}(t)$ represents the maximum number of vehicles entering into cell i at time t. $N_i(t)$ represents the maximum number of vehicles stored in cell i at time t. v and w are the free-flow and shockwave speeds, respectively. The q-k fundamental diagram can be depicted as Figure 1(a).

In this paper, to facilitate CTM to simulate traffic behaviors at the incident site where the capacity is reduced and the traffic speed is restricted within the speed limits due to lane-closure, the q-k diagram is further revised accordingly as depicted in Figure 1(b). As shown in Figure 1(b), jam density (i.e., maximum storage capacity, $N_i(t)$) will be reduced from k_j to θk_j, where θ ($0 \le \theta \le 1$) denotes the percentage of lanes remaining for traffic. For instance, $\theta = 2/3$ indicates one-lane closure on a three-lane freeway because 1/3 of storage capacity is blocked and unable to store any vehicles. Furthermore, once partial lanes are closed the capacity (maximum flow rate) will be dropped from q_m to ρq_m, where ρ ($0 \le \rho \le 1$) denotes the remaining capacity ratio. Table 1 reports the ρ values observed from a field survey in Taiwan. As expected, ρ is smaller than θ because the closely interacting movements of merging traffic upstream of the incident can further reduce the maximum outflow rate.

Table 1. The capacity ratio and jam density ratio remaining under various lane closure conditions.

Number of lanes	Number of lanes closure	Capacity reduction ratio (%)	Capacity ratio remained (ρ)	Jam density ratio remained (θ)
2	1	63.3	36.7	50.0
3	2	76.2	23.8	33.3
3	1	56.2	43.8	66.7
4	3	82.8	17.2	25.0
4	2	68.2	31.8	50.0
4	1	49.8	50.2	75.0

Source: Chen (1991).

Based on the capacity ratio and jam density ratio remaining, the q-k diagram can be determined by further assuming both free-flow and shockwave speeds unchanged. The traffic movements are governed by different q-k diagrams, depending on their locations along the freeway upstream of the incident. The traffic movement rules in Equations (3) and (4) are revised as following equations:

$$y_i(t) = \min\{n_{i-1}(t), \rho q_{mi}(t), \beta[\theta N_i(t) - n_i(t)]\}, \tag{5}$$

Downloaded by [National Chiao Tung University] at 14:21 28 April 2014

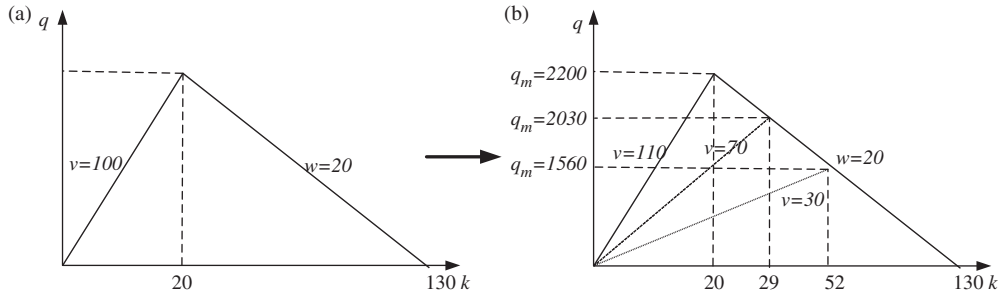

Figure 2. *q-k* diagrams for (a) normal and (b) variable speed-limit controlled segments.

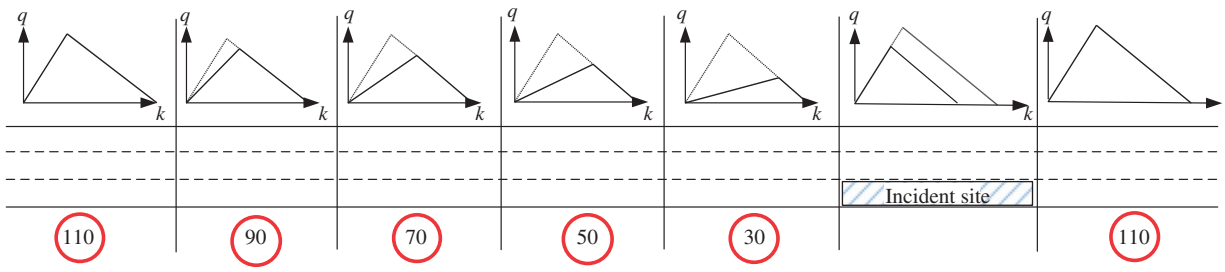

Figure 3. *q-k* diagrams under VSL control.

$$\beta = \begin{cases} 1, & n_{i-1}(t) \le \rho q_{mi}(t) \\ \dfrac{w}{v}, & n_{i-1}(t) \ge \rho q_{mi}(t) \end{cases}. \tag{6}$$

To reflect the effects of VSL control on traffic movements, the *q-k* diagrams in different cells of the VSL controlled segment will be revised as depicted in Figure 2. Here, free-flow speed is revised in accordance with variable speed limits; and capacities of different cells of the VSL segment are changed via a simple geometric triangular relationship. It is worth noting that the *q-k* diagram depicted in Figure 2(b) is valid only for the condition of perfect obedience by drivers to VSL control. For the condition of partial obedience, the traffic behavior is much more complicated to accurately simulate without field observations. Moreover, conditions where some drivers obey the controlled speed limit and others do not result in significantly inconsistent driving behavior among drivers in the traffic and be even more hazardous than without VSL control. Thus, the implementation of VSL control should be coupled with strict speed limit enforcement, for example, one should equip VSL signs with speed cameras, and strong promotion of drivers' education, to encourage familiarity with VSL control measures.

For example, for a speed limit increment of 20 km/h and an average speed of 30 km/h at the incident site, the *q-k* diagrams along the study corridor are depicted in Figure 3, where the traffic movement rules are revised as follows:

$$y_i(t) = \min\{n_{i-1}(t), \rho' q_{mi}(t), \beta[N_i(t) - n_i(t)]\}, \tag{7}$$

$$\beta = \begin{cases} 1, & n_{i-1}(t) \le \rho' q_{mi}(t) \\ \dfrac{w}{\gamma v}, & n_{i-1}(t) \ge \rho' q_{mi}(t) \end{cases}, \tag{8}$$

where γ is the reduced speed limit ratio, and $\rho' q_{mi}$ denotes the remaining capacity at cell i due to corresponding controlled speed limit ($0 \le \rho' \le 1$).

3. Validation of revised cell transmissions model

To validate the revised CTM in replicating the freeway traffic behavior in Taiwan under various traffic conditions, five sets of real traffic data were collected from Taiwan's freeways. The upstream traffic data are set as the input flow of CTM and the detected traffic data at the downstream site of interest are used to validate the accuracy of the revised CTM. The results are respectively given in the following.

(1) *Basic segment under free flow*: the selected study corridor is located at a three-lane basic segment from 141 + 2 K to 143 + 4 K southbound

Downloaded by [National Chiao Tung University] at 14:21 28 April 2014

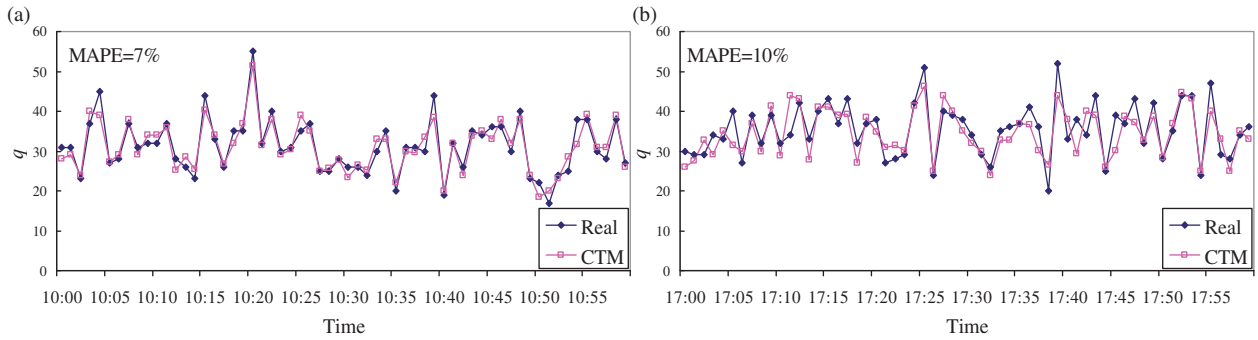

Figure 4. Validation results of revised CTM under free-flow condition: (a) basic segment and (b) weaving segment.

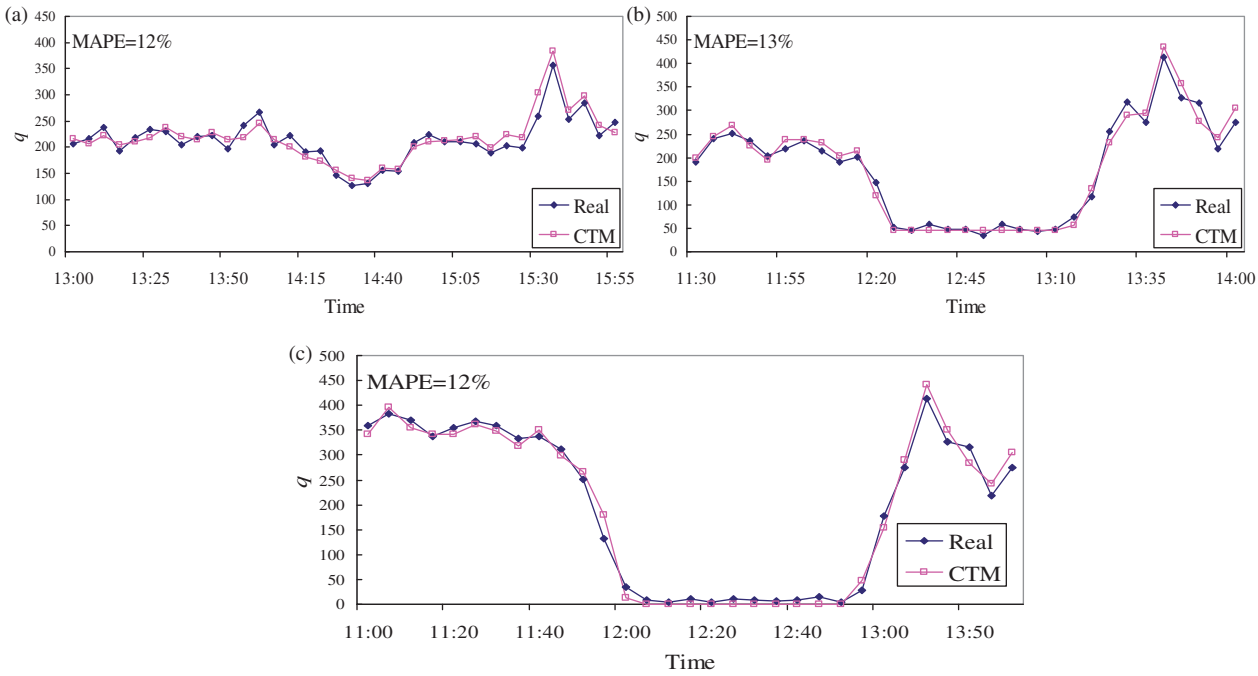

Figure 5. Validation results of revised CTM under congested flow condition: (a) one-lane closure, (b) two-lane closure, and (c) three-lane closure.

(a length of 2.2 km) on Freeway No.3. The validation result is depicted in Figure 4(a) with a MAPE (mean absolute percentage error) of 7%.

(2) *Weaving segment under free flow*: the selected study corridor is located at a three-lane weaving segment from 174 + 9 K to 177 + 1 K southbound (a length of 2.2 km) on Freeway No.3. The validation result is depicted in Figure 4(b) with a MAPE of 10%.

(3) *One-lane closure under congested condition*: the selected study corridor is located at a three-lane basic segment from 198 + 6 K to 197 + 1 K northbound (a length of 1.5 km) on Freeway No.1. An incident occurs at 197+9 K causing one-lane closure with duration of approximately 1.3 h (from 14:00 to 15:30). The validation result is depicted in Figure 5(a) with a MAPE of 12%.

(4) *Two-lane closure under congested flow*: the selected study corridor is located at a three-lane basic segment from 168 + 1 K to 166 + 8 K northbound (a length of 1.3 km) on Freeway No. 1. An incident occurs at 167+0 K causing two-lane closure with duration of approximately 1.1 h (from 12:20 to 13:30). The validation result is depicted in Figure 5(b) with a MAPE of 13%.

Downloaded by [National Chiao Tung University] at 14:21 28 April 2014

(5) *Three-lane closure under congested flow*: the selected study corridor is located at a three-lane basic segment from 110 + 0 K to 113 + 4 K southbound (a length of 3.4 km) on Freeway No. 1. An incident occurs at 111+2 K causing three-lane closure with duration of approximately 2.0 h (from 11:40 to 13:40). The validation result is depicted in Figure 5(c) with a MAPE of 12%.

The above-mentioned five cases show that our revised CTM, together with the revised *q*-*k* diagrams, is able to satisfactorily replicate the traffic behavior at the incident sites.

4. Evaluation of model performance

4.1. *Model training*

To facilitate the learning of the proposed GFLC-based VSL control model, this study collected two sets of accident-free 1-min traffic data from Freeway No.1, both contain 1.5 h of peak (low speed) and off-peak (medium-to-high speed). We used these two traffic conditions as the upstream traffic inflows for the revised CTM. Three severity degrees of incidents are given to simulate the downstream traffic. Each incident will last for 30 min. In addition, 30 min before and after the incident are also simulated. It makes a total of six cases: one-lane closure (slight incident), two-lane closure (moderate incident), and three-lane closure (severe incident) under peak (heavy traffic) and off-peak (light traffic) conditions. Note that the three-lane closure represents an incident of the highest severity because all lanes are blocked in this three-lane freeway context. The proposed model aims to learn the optimal combination of logic rules and membership functions through the six cases. With the optimally selected fuzzy logic rules and tuned membership functions, the proposed GFLC model can determine an optimal speed limit increment based on real-time traffic conditions and incident severity.

The parameters of the proposed model are set the same as those in Chiou and Lan (2005). The weight of CL is set as: $\alpha = 0.5$. Each time click of CTM is set as 6 s and the length of cell is set as 183 m. The proposed model updates the optimal speed-limit increment every 5 min. Besides, we assume that all state/control variables are within five linguistic degrees, each represented by a triangle membership function. This makes a total of 625 potential logic rules. With one gene for each rule, there would be 125 genes in a chromosome; thus, a total of 36 position parameters are to be calibrated for tuning the membership functions. With four genes for each parameter, there would be 144 genes in a chromosome.

Table 2. Information of six incident cases.

Traffic flow condition	Severity of incident (number of lanes closure)	Incident site on Freeway No.1 (three-lane mainline)	Incident duration (minutes)
Off-peak (light flow)	1	200.6 K southbound	31
	2	191.9 K southbound	47
	3	139.8 K northbound	59
Peak (heavy flow)	1	197.9 K northbound	38
	2	167.0 K northbound	52
	3	111.2 K southbound	63

4.2. *Model performance*

To evaluate the performance of the proposed model, six incident cases which occurred on Freeway No.1 were investigated, as shown in Table 2. These incident cases represented slight (one-lane closure), moderate (two-lane closure), and severe (all-lane closure) incidents under both free-flow and congested-flow conditions. Their corresponding 1-min traffic data, including mainline, on-ramp, and off-ramp within the 15 km upstream of the incident sites, were also collected and used as the inflows of the revised CTM.

The control performances of the proposed model and the non-VSL (serving as baseline) are presented in Table 3. Compared with non-VSL control, the proposed model can improve safety (CL) from 1.02% to 14.49% at no expense to or slight decrease in throughput (TT) by up to 2.24%. In terms of crash likelihood reduction, the proposed model performs better in the cases of less severe incidents (e.g., one-lane closure) and peak hours. It is because the interactions among vehicles become more prevalent as traffic volume increases. Lowering the speed limits can effectively avoid seriously negative interactions among vehicles in different cells. In the cases of severe incidents with more lanes closure, all upstream cells may exhibit very similar traffic conditions, that is, gridlock, soon after the incident occurs. This will make the VLS control less effective. In addition to the safety enhancement, it is interesting to note that the proposed model did not adversely affect the throughput (e.g., for three-lane closure under either off-peak or peak hours).

Table 4 displays the variable speed limits upstream of six incident sites at the moment when the incidents occur. It should be mentioned that the displayed speed

Downloaded by [National Chiao Tung University] at 14:21 28 April 2014

Table 3. Performance of the proposed VSL control model.

Traffic flow condition	Severity of incident (number of lanes closure)	Index	Non-VSL (baseline)	VSL model	Improvement rate (%)	Evaluation period (minutes)
Off-peak (light flow)	1	*CL*	497	462	**7.04**	91
		TT	2956	2918	−1.29	
	2	*CL*	1549	1466	**5.36**	107
		TT	2645	2621	−0.91	
	3	*CL*	3120	3071	**1.57**	119
		TT	2078	2078	0.00	
Peak (heavy flow)	1	*CL*	5295	4528	**14.49**	98
		TT	5054	4941	−2.24	
	2	*CL*	13,048	11,724	**10.15**	112
		TT	4386	4303	−1.89	
	3	*CL*	15,994	15,831	**1.02**	123
		TT	3652	3652	0.00	

Table 4. Variable speed limits displayed upstream of six incident sites.

Traffic flow condition	Severity of incident (Number of lanes closure)	Optimal speed-limit increment (kph)	Variable speed limits displayed						
Off-peak (light flow)	1	10		110	100	90	80	70	60
	2	20			110	100	80	60	40
	3	20	110	100	80	60	40	20	0
Peak (heavy flow)	1	20				110	90	70	50
	2	30				110	80	50	20
	3	40				110	80	40	0

limit on each sign can differ as time evolves during the period of an incident, depending on the average speed at the incident site and the updated incident information. For every 5 min, the GFLC model will automatically determine a new speed-limit increment according to real-time state variables status based on the selected fuzzy rules and tuned membership functions. The speed limit of the nearest VSL sign is automatically determined by the average speed of the incident site. With the determined speed-limit increment and average speed of traffic at the incident site, the displayed speed limits of upstream VSL signs can then be decided.

Basically, the speed-limit increment should be kept as small as possible to eliminate any potential shockwaves if only the safety index is considered. However, for the case of a severe incident under heavy traffic, a small speed-limit increment means a wide

Downloaded by [National Chiao Tung University] at 14:21 28 April 2014

Table 5. Performances of the proposed model under various values of α.

Off-peak/peak	Number of lanes blocked	Indices	α										
			0.0	0.1	0.2	0.3	0.4	0.5	0.6	0.7	0.8	0.9	1.0
Off-peak (light flow)	1	*CL*	522	516	508	495	482	474	470	462	453	432	419
		TT	2638	2614	2610	2594	2581	2572	2561	2554	2530	2524	2521
	2	*CL*	1553	1534	1511	1493	1487	1466	1441	1428	1416	1403	1376
		TT	2703	2689	2675	2659	2637	2623	2616	2611	2594	2581	2561
	3	*CL*	3248	3201	3168	3134	3097	3071	3002	2989	2976	2968	2933
		TT	2198	2167	2135	2104	2088	2078	2061	2049	2033	2028	2014
Peak (heavy flow)	1	*CL*	4798	4736	4688	4633	4579	4528	4501	4486	4471	4458	4421
		TT	5087	5064	5030	5006	4988	4959	4944	4928	4920	4913	4909
	2	*CL*	12684	12596	12438	12111	11985	11724	11563	11410	11268	11200	11123
		TT	4589	4501	4435	4399	4321	4296	4203	4176	4158	4146	4122
	3	*CL*	17023	16823	16256	16003	15999	15917	15832	15773	15700	15623	15546
		TT	3899	3802	3765	3722	3687	3652	3602	3580	3566	3559	3538

Table 6. Performances of the proposed model under various VSL deployment densities.

Peak/off-peak	Number of lanes closed	Performance indices	Deployment density of VSL signs		
			1 km	2 km	3 km
Off-peak (light flow)	1	CL	497	530	564
		TT	2956	2834	2953
	2	CL	1549	1561	1604
		TT	2645	2573	2612
	3	CL	3120	3156	3222
		TT	2078	2070	2041
Peak (heavy flow)	1	CL	5295	5455	5585
		TT	5054	4895	4933
	2	CL	13,048	13,198	13,455
		TT	4386	4313	4343
	3	CL	15,994	16,134	16,386
		TT	3652	3639	3629

upstream roadway area should be VSL controlled, which certainly will reduce traffic throughput. Therefore, as shown in Table 4, our proposed model tends to determine a larger speed-limit increment under severe incidents and heavy traffic flow conditions in order to minimize the controlled area.

4.3. *Sensitivity analysis*

To further investigate the effects of various values of α on the control performance, a sensitivity analysis on the value of α is conducted as shown in Table 5. The results consistently show that as the value of α increases, the traffic under VSL control becomes safer with a lower *CL* value but less efficient with a lower *TT* value, indicating a trade-off relationship between safety and efficiency.

This paper assumes that VSL signs are equally spaced every 1 km. To further examine the effects of different VSL deployment densities, the performances of deployment densities of every 2 and 3 km are compared in Table 6. Note that the values of CL consistently increase as the density of VSL decreases, suggesting denser deployment of VSL signs is beneficial to safety.

Interestingly, the trend of changes in TT is not consistent. For the cases of one- or two-lane closure, the deployment density of every 2 km presents the lowest TT. In contrast, for the cases of three-lane closure during peak and off-peak periods, the deployment density of every 3 km has the lowest TT.

Downloaded by [National Chiao Tung University] at 14:21 28 April 2014

Downloaded by [National Chiao Tung University] at 14:21 28 April 2014

However, for all cases, the deployment density of every 1 km achieves the highest TT.

Although the above results consistently show that the deployment density of every 1 km performs best in terms of safety and efficiency, the implication can not be extended to the scenarios of higher deployment densities. It is because dense deployment of VSL signs may confuse drivers and lower their degrees of obedience to VSL signs. The driver response to VSL signs, including degree of obedience and perception-response time which are not considered in the proposed model, deserves a further field study.

5. Concluding remarks

This paper has developed a GFLC-based VSL control model. The proposed VSL control model performance is evaluated with consideration of both crash likelihood and throughput efficiency. To facilitate the learning process of GFLC, a revised CTM was proposed to efficiently simulate traffic behavior. The results of different incident cases have shown that the proposed VSL control model can effectively curtail the crash likelihood without decreasing or only slightly decreasing the throughput efficiency. It suggests that our proposed VSL control model is promising for better managing of incidents, particularly in the context of intelligent highway systems wherein VSL signs are densely installed.

Several directions for future studies can be identified. First, the crash likelihood proposed by Abdey-Aty *et al*. (2005) should be measured at a microscopic level, where the speed of individual vehicle in the system should be simulated. However, it is not possible for a mesoscopic traffic simulator like CTM to delivery such detailed information. Instead, this study used the average spatiotemporal speeds of cells (i.e., a group of vehicles) to replace the individual vehicle speeds. We believe that the crash likelihood must be underestimated since the speed variations among vehicles in each cell was assumed zero. Therefore, it is worth developing a crash likelihood function at a mesoscopic level or a more efficient genetic learning algorithm based on a microscopic traffic simulation model. Second, to simplify the control strategy, the VSL signs are assumed equally spaced over the incident upstream stretch and the increment of speed limits for the sequential VSL signs is assumed constant. Obviously, these assumptions may not be practical. Therefore, more complex VSL control strategies deserve to be explored. Third, to cross-validate the effectiveness of the proposed model, a microscopic traffic simulator may be used to evaluate the performance of the logic rules and membership functions learned from our revised CTM mesoscopic model. Fourth, the percentage of capacity reduction due to lane-closure requires further investigation to obtain a more correct q-k relationship in order to enhance the accuracy of revised CTM. Last but not least, the performance of VSL control mainly depends upon the degree of obedience by drivers to the controlled speed limit. This paper assumes all drivers will perfectly obey the controlled speed limit. The assumption is valid only for the VSL conditions which involve strict enforcement of speeding regulations and drivers' close familiarity with VSL control devices. Therefore, the performance of a VSL control strategy under low obedience and significant response delay time deserves an in-depth investigation.

Acknowledgments

The authors wish to thank two anonymous referees for their insightful comments and constructive suggestions.

Nomenclature

CL	crash likelihood
TT	total vehicle throughput
a	weight of CL representing the relative importance of safety over efficiency
$n_i(t)$	the number of vehicles in cell i at time t
$y_i(t)$	the number of vehicles flowing into cell i at time t
$q_{mi}(t)$	the maximum number of vehicles entering into cell i at time t
$N_i(t)$	the maximum number of vehicles stored in cell i at time t
v	free-flow speed
w	shockwave speed
ρ	capacity ratio remained
θ	jam density ratio remained
γ	the reduced speed limit ratio
$\rho' q_{mi}$	the remaining capacity at cell i due to corresponding controlled speed limit

References

Abdey-Aty, M., Dilmore, J., and Dhindsa, A., 2006. Evaluation of variable speed limits for real-time freeway safety improvement. *Accident analysis and prevention*, 38 (2), 335–345.

Abdel-Aty, M., Uddin, N., and Pande, A., 2005. Split models for predicting multi-vehicle crashes during high-speed and low-speed operating conditions on freeways. *Transportation research record: journal of the transportation research board*, 1908 (1908), 51–58.

Breton, P. *et al*., 2002. Shock wave elimination/reduction by optimal coordination of variable speed-limits. *In: Proceedings of the IEEE 5th international conference on intelligent transportation systems (ITSC'02)*, Singapore, 225–230.

Chen, Z.H., 1991. *Exploring the characteristics of saturated flow and capacity on incident-induced freeway traffic controlled segments*. Thesis (Masters), National Cheng Kung University, Tainan, Taiwan (In Chinese).

Chiou, Y.C. and Lan, L.W., 2005. Genetic fuzzy logic controller: an iterative evolution algorithm with new encoding method. *Fuzzy sets and systems*, 52 (3), 617–635.

Daganzo, C.F., 1994. The cell transmission model: a dynamic representation of highway traffic consistent with the hydrodynamic theory. *Transportation research*, 28B (4), 269–287.

Daganzo, C.F., 1995. The cell transmission model: network traffic. *Transportation research*, 29B (4), 79–93.

Kang, K.P. and Chang, G.L., 2006. A robust model for optimal time-of-day speed control at highway work zones. *IEEE transactions on intelligent transportation systems*, 7 (1), 115–123.

Hegyi, A., De Schutter, B., and Hellendoorn, J., 2005. Model predictive control for optimal coordination of ramp metering and variable speed-limits. *Transportation research*, 13C (3), 185–209.

Lee, C., Hellinga, B., and Saccomanno, F., 2004. Assessing safety benefits of variable speed-limits. *Transportation research record: journal of the transportation research board*, 1897, 183–190.

Lee, C., Hellinga, B., and Saccomanno, F., 2006. Evaluation of variable speed limits to improve traffic safety. *Transportation research*, 14C (3), 213–228.

Lin, P.W., Kang, K.P., and Chang, G.L., 2004. Exploring the effectiveness of variable speed limit controls on highway work-zone operations. *Intelligent transportation systems*, 8 (3), 155–168.

Yadlapati, S.S., and Park, B.B., 2004. *Development and testing of variable speed limit control logics for work zones using simulation*. Virginia, USA: University of Virginia, Research report of the University of Virginia, No. UVACTS-13-0-43.

Downloaded by [National Chiao Tung University] at 14:21 28 April 2014